

Structural composition dependence of amorphous silicon-iron prepared by ion implantation and by coevaporation: A Mössbauer study

F. H. Sánchez, M. B. Fernández van Raap, and J. Desimoni

*Departamento de Física, Facultad de Ciencias Exactas, Universidad Nacional de La Plata,
Casilla de Correo No. 67, 1900 La Plata, Buenos Aires, Argentina*

(Received 4 October 1990)

The structural evolution of amorphous $\text{Si}_{1-x}\text{Fe}_x$ with composition has been investigated. Implanted specimens with iron concentrations below and above $x=0.2$, where a structural transformation was previously reported for evaporated samples, have been studied by conversion-electron Mössbauer spectroscopy. Applying the model of Miedema and van der Woude for the isomer shift, a consistent description of our results and of those available from the literature (both from ion-implanted and coevaporated specimens) is given, which covers a wide composition range ($0.001 \leq x \leq 0.750$). It was concluded that three differentiated regions exist: a silicon-rich one where iron bears a strong covalent character in a continuous random network structure; an intermediate region where the covalent character decreases continuously at the iron sites, which are here proposed to have a local structure like the one existing in the intermetallic compound FeSi; and finally an iron-rich region where covalent effects are absent, supporting a dense-random-packing description of the amorphous structure.

INTRODUCTION

Iron-implanted silicon has been studied for the past 20 years,¹⁻⁵ but questions concerning the nature of the implanted atoms surroundings and the origin of the hyperfine interactions observed at the iron nuclei still remain. Furthermore, fundamental aspects regarding the structure of the system versus iron concentration have not been sufficiently clarified.

Nevertheless, important information has been gained from these studies. It is well known that for implantation energies around 100 keV, the system amorphizes in a continuous-random-network (CRN) structure when the dose exceeds 10^{14} Fe atoms/cm². It has been also proved that there exists a nonzero electric-field gradient at the Fe nucleus, which causes the appearance of an asymmetric doublet in the ⁵⁷Fe Mössbauer spectra, and that this electric-field gradient does not differ too much from site to site in the amorphous network.^{6,7} Indeed, this situation persists in a wide composition range. Mössbauer studies performed in the $\text{Si}_{1-x}\text{Fe}_x$ system have shown that both the ⁵⁷Fe quadrupole splitting (Δ_{QS}) and isomer shift (δ_{IS}) change only smoothly in the $0.001 \leq x \leq 0.167$ (Ref. 1) range.

On the other hand, electron-diffraction studies carried out in amorphous $\text{Si}_{1-x}\text{Fe}_x$ thin films prepared by evaporation indicate the formation of two different amorphous structures depending on the composition.⁸ For $x < 0.20$, a CRN structure has been found, whereas a dense-random-packing (DRP) short-range order has been observed above this iron concentration.

It has been recently demonstrated by Rutherford back-scattering spectrometry (RBS) that maximum iron concentrations of up to $x \cong 0.63$ can be obtained by means of Fe ion implantation into Si.⁹ In addition, Read camera x-ray-diffraction studies performed on room temperature

(RT) implanted samples have shown no signs of crystalline phase formation, at least up to $x=0.4$.¹⁰

To our knowledge no Mössbauer studies have been undertaken so far on silicon implanted with iron to concentrations beyond $x=0.17$. In order to investigate whether a CRN-DRP-type structural change occurs also at $x \cong 0.2$ in the $\text{Si}_{1-x}\text{Fe}_x$ system prepared by ion implantation, we have performed Mössbauer studies on samples produced by this technique with compositions in the range $0.16 \leq x \leq 0.39$. Our results indicate that indeed the short-range order around the iron sites begins to change above $x \cong 0.17$. Based on the model of Miedema and van der Woude¹¹ for the δ_{IS} , we conclude that from this composition onwards the system evolves from semiconductor to metallic. This transformation is not complete until x reaches a value of about 0.5.

EXPERIMENT

Polished Si single-crystal wafers with (100) orientation have been implanted with 150-keV Fe^+ ions at a pressure of less than 10^{-6} Torr using the Varian DF4 facility of the Physics Department of the University of Connecticut.

Due to the insufficient resolution for the accelerator mass separator, the ⁵⁷Fe⁺ beam has been obtained from existing noble-metal Fe alloys made from 80 at. % ⁵⁷Fe enriched iron. The Fe concentration has been built up by alternatively exposing the Si targets to the ⁵⁷Fe⁺ beam and to a ⁵⁶Fe⁺ beam generated from a natural iron source. This process was accomplished in several steps in order to avoid differences in the final location and distribution of ⁵⁶Fe and ⁵⁷Fe atoms. The beams have been scanned both in the horizontal and vertical directions to ensure lateral uniformity of the samples composition.

RBS characterization of the implanted specimens has been performed employing a 1.5-MeV He^+ beam at the

2-MeV Van der Graaff accelerator of the Institute of Materials Science of the University of Connecticut.

The implanted samples have been checked for the formation of crystalline Fe-Si phases performing grazing x-ray-diffraction (Read camera) experiments. No evidence for crystalline reflections other than from the Si single-crystal substrates has been observed.

The Mössbauer experiments have been carried out in a conventional constant acceleration spectrometer at the Physics Department of the University of La Plata. A 25-mCi $^{57}\text{CoRh}$ source was used to obtain the 14.4-keV γ rays of the main Mössbauer transition of ^{57}Fe . The conversion (and Auger) electrons originated during the decay of the resonant ^{57}Fe nuclei in the absorbers (implanted samples) have been detected with a He-94%–methane-6% gas admixture flux detector in which samples had been electrically attached to the cathode. The analysis of the Mössbauer spectra has been performed with a conventional nonlinear least-squares-fitting routine employing Lorentzian functions.

Thermal treatments have been carried out in a conventional electric oven with samples encapsulated in quartz tubes under pressures below 10^{-3} Torr.

RESULTS AND DISCUSSION

Figure 1 shows the RBS spectra of the samples implanted with minimum and maximum fluences, designed by *A* and *D*, respectively. Effects of sputtering-induced saturation and perhaps of radiation-enhanced diffusion may be inferred from the flat top and large width of the iron peak of the most heavily implanted sample (*D*). The composition of these samples as a function of depth (*z*) is displayed in Fig. 2.

Since the Mössbauer spectra come from a superposition of signals originated with the same probability at every probe nucleus, the observed hyperfine interactions $Y(v)$ (for relative source-absorber velocity v) correspond to an average obtained by weighting the mean Mössbauer signal at depth z , $Y(z, v)$, with the iron atomic fraction $x'(z)$, $Y(v) = \int Y(z, v)x'(z)dz / \int x'(z)dz$. This is so because the number of ^{57}Fe nuclei probing such surround-

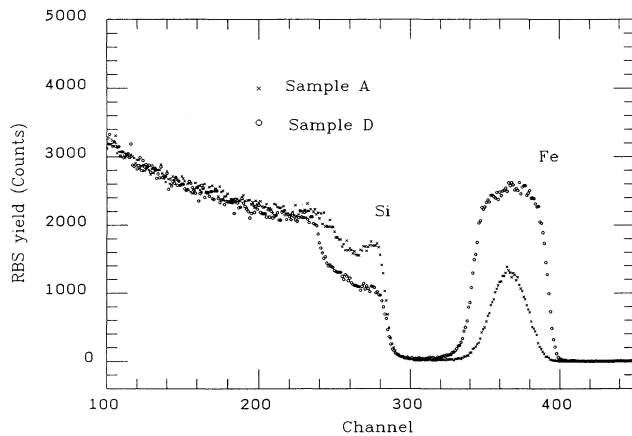


FIG. 1. 1.5-MeV He^+ RBS spectra of Si samples implanted with the lowest (*A*) and highest (*D*) Fe fluences.

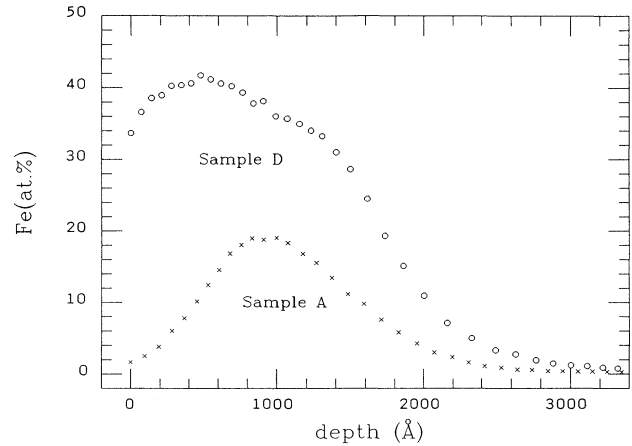


FIG. 2. Depth dependence of the Fe atomic concentration for the samples implanted with the lowest (*A*) and highest (*D*) Fe fluences, deduced from the RBS data (Fig. 1). The system atomic density has been calculated as the weighted average of those of the pure elements (Si and Fe).

ings scales with $x'(z)$. Accordingly, the mean iron concentration x associated with each Mössbauer spectrum has been then calculated by $x = \int (x')^2(z)dz / \int x'(z)dz$.

The Mössbauer spectra of samples *A* and *D* are shown in Fig. 3. In agreement with previous studies each spectrum consists of a broadened and symmetric quadrupole doublet. In Table I, the Mössbauer parameters obtained from the best least-squares fits of theoretical functions to the experimental data are listed, along with the mean concentrations x for samples *A*–*D*.

As shown in Fig. 4, the δ_{IS} and Δ_{QS} values for $x \approx 0.17$ fit well with data previously obtained in the range $0.001 \leq x \leq 0.167$.¹ These data show an approximately linear diminution of both quantities with the logarithm of x in this region. On the other hand, the rest of our data

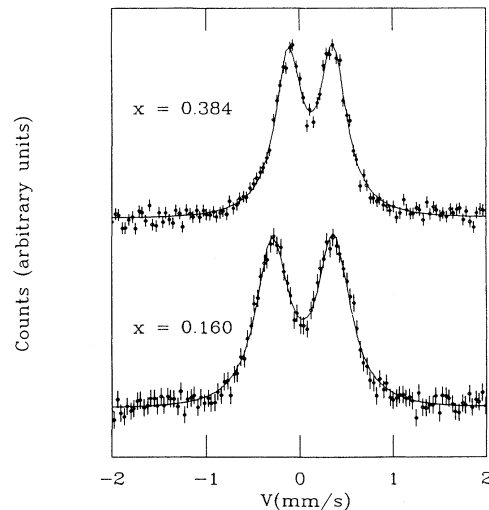


FIG. 3. Mössbauer spectra corresponding to samples implanted with lowest ($x=0.160$) and highest ($x=0.384$) Fe fluences.

TABLE I. Average Fe atomic fraction x , isomer shift δ_{IS} (relative to bcc iron), quadrupole splitting Δ_{QS} , relative area of second to first doublet component S_2/S_1 , and Lorentzian linewidth Γ , for samples measured in this work.

Sample	x	δ_{IS} (mm/s)	Δ_{QS} (mm/s)	S_2/S_1	Γ (mm/s)
A	0.160	0.119(5)	0.653(9)	0.98(4)	0.393(13)
B	0.171	0.131(4)	0.622(7)	0.98(3)	0.391(11)
C	0.367	0.204(4)	0.545(6)	1.01(3)	0.375(9)
D	0.384	0.229(3)	0.478(4)	0.98(2)	0.349(7)

reveal that a noticeable change occurs above $x \cong 0.17$. The δ_{IS} begins to increase whereas the Δ_{QS} decreases more rapidly. This change could be interpreted as produced by a structural modification of the amorphous phase. The correlation between δ_{IS} and Δ_{QS} and the transition at $x=0.17$ are more clearly observed in a $\delta_{\text{IS}}-\Delta_{\text{QS}}$ plot (Fig. 5). In this representation any uncertainty in x (due for instance to differences between the estimated and actual distribution of implanted atoms, composition heterogeneity, etc.) should be wiped out, enabling a more accurate experimental correlation between experimentally measured quantities in the amorphous system and its crystalline counterparts.

Mangin *et al.*⁸ have observed a modification of the electron-diffraction pattern taken from evaporated amorphous $\text{Si}_{1-x}\text{Fe}_x$ films at $x \cong 0.2$, which they interpreted as a transition from a CRN to a DRP structure. If the amorphous phases prepared by this means and by ion implantation do not differ appreciably, the same structural transformation would be responsible for the behavior of the δ_{IS} and Δ_{QS} shown in Fig. 4. In fact, results obtained from evaporated amorphous films,^{12,13} do not disagree with the overall δ_{IS} evolution (see Fig. 6). (Unfortunately, Marchal *et al.*¹² have not reported on their Δ_{QS} data).

Let us discuss first the δ_{IS} data in the low x concentration range. Both the δ_{IS} sign and its decreasing behavior are expected from previous experimental studies¹⁴⁻¹⁶ as

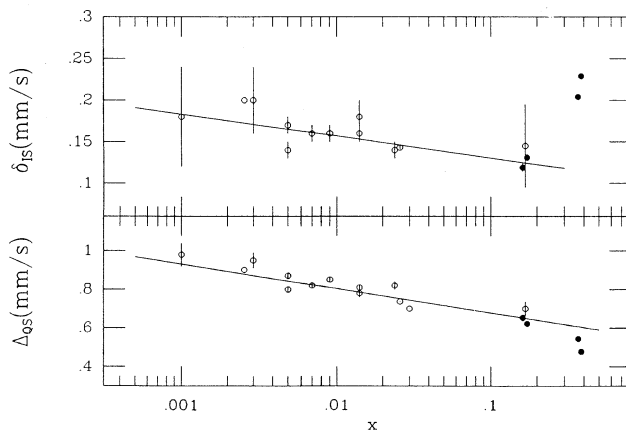


FIG. 4. Isomer shift and quadrupole splitting data obtained from iron-implanted silicon samples as a function of the average Fe atomic fraction x . Open circles are the results from Refs. 1 and 3-5; solid circles are from present work.

well as from semiempirical approaches.¹⁷ As Ingalls, van der Woude, and Sawatzky have pointed out,¹⁸ the variation in ^{57}Fe δ_{IS} is in many systems approximately additive with the number of near neighbors of a given class. Thus, since near-neighbor silicons produce positive shifts, by increasing x we should observe a δ_{IS} diminution. Furthermore, in an amorphous system we would not need to care about atomic volume effects, since it will be no restrictions on this quantity imposed by the host structure.¹⁷ This assumption is supported by the results of isochronal annealing performed on the $x=0.16$ sample up to temperatures of 973 K, which induced almost no change in the δ_{IS} value (Table II) indicating no structural relaxation effects on this magnitude.

On the other hand, the detailed dependence of the δ_{IS} on x is less clear. Proposed models state a linear or quasilinear x dependence for ideal solution systems.^{17,18} A departure from the linear regime could be imagined if

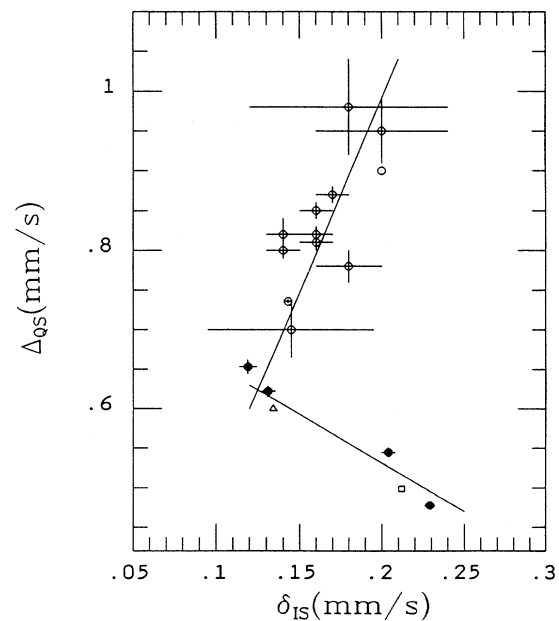


FIG. 5. Correlation between quadrupole splitting Δ_{QS} and isomer shift δ_{IS} in Fe-implanted Si samples. Open circles correspond to $x \leq 0.167$ (Refs. 1 and 3-5) and solid circles correspond to $0.160 \leq x \leq 0.384$ (this work). The figure also shows the results from an $x \cong 0.3$ evaporated thin-film sample (triangle, Ref. 13), and from the intermetallic compound FeSi (square, Ref. 22).

TABLE II. Isomer shift δ_{IS} (relative to bcc iron), quadrupole splitting Δ_{QS} , relative area S_2/S_1 , and Lorentzian linewidth Γ for sample A ($x=0.160$), after annealings performed during a time t at temperature T .

T (K)	t (min)	δ_{IS} (mm/s)	Δ_{QS} (mm/s)	S_2/S_1	Γ (mm/s)
RT (as implanted)		0.119(5)	0.653(9)	0.98(4)	0.393(13)
573	30	0.141(3)	0.661(5)	0.97(2)	0.423(8)
673	30	0.143(5)	0.678(9)	1.04(4)	0.407(13)
773	30	0.123(8)	0.527(12)	1.22(7)	0.423(19)
873	30	0.094(2)	0.437(3)	0.99(2)	0.310(5)
973	30	0.098(9)	0.425(5)	0.98(3)	0.313(9)

local composition around Fe probes differs markedly from the average value due, for instance, to preferential Fe-Fe association. In such a case, the number of Fe near neighbors to a ^{57}Fe probe would be an increasing function of x with a decreasing slope resembling somehow the logarithmic function shape. However, under the assumption that the electric-field gradient is essentially produced by the fixed point charges, this situation would imply an increase of the Δ_{QS} with x instead of the experimentally observed decreasing behavior. On the other hand, an electric-field gradient contribution originated at the iron electron shell, which could be increasingly canceled by the fixed charges contribution, appears to be excluded by the small temperature dependence reported for the Δ_{QS} .¹⁹

Sawicka *et al.*¹⁹ have proposed that in the $x \leq 0.17$ range, Fe atoms may act as vacancy traps and subsequently form extended defects around the probes. They also suggested that by this means tetrahedral bonding would be disrupted in those regions, which would be

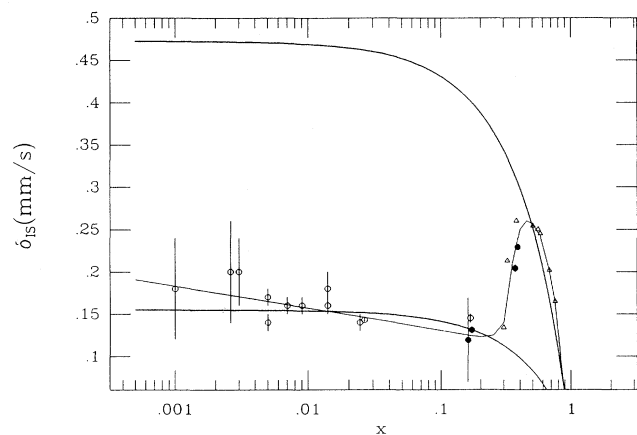


FIG. 6. Analysis of the $\text{Si}_{1-x}\text{Fe}_x$ system with the model of Miedema and van der Woude for the Mössbauer isomer shift. Open circles (Refs. 1 and 3–5) and solid ones (present work) correspond to implanted samples. Triangles (Refs. 12 and 13) correspond to coevaporated systems. The upper heavy curve is the composition dependence prediction using the model parameters obtained by van der Kraan and Buschow for metallic amorphous iron alloys [which in turn determine the infinitely diluted limit $\delta_{IS_{\max}} = \delta_{IS}(x=0)$]. The lower bold curve constitutes the best fit of Eq. (1) to the low iron composition range data ($x \leq 0.17$) having set free the parameter $\delta_{IS_{\max}}$. The light curve is to guide the eye through the experimental data points.

larger the higher the iron concentration thus producing complexes of increasing symmetry with the consequent Δ_{QS} reduction. While this mechanism could be considered in the explanation of the δ_{IS} and Δ_{QS} evolution for $x > 0.17$, an examination of the experimental δ_{IS} data with the model of Miedema and van der Woude¹¹ seems to rule out bond breaking, at least to an important extent, in the low-iron-concentration region as we shall see next. In this model,

$$\delta_{IS}(x) = C_s^{\text{Si}}(x) \delta_{IS_{\max}}, \quad (1)$$

$$C_s^{\text{Si}}(x) = (1-x)V_{\text{Si}}^{2/3} [xV_{\text{Fe}}^{2/3} + (1-x)V_{\text{Si}}^{2/3}]^{-1},$$

$$\delta_{IS_{\max}} = P'(\phi_{\text{Si}}^* - \phi_{\text{Fe}}^*) + Q'(n_{\text{WS}}^{\text{Si}} - n_{\text{WS}}^{\text{Fe}})/n_{\text{WS}}, \quad (2)$$

where the δ_{IS} is referred to bcc iron and ϕ^* , n_{WS} , and V are the work function, the electronic density at the boundary of the Wigner Seitz cell, and the molar volume of each element.²⁰ Taking the values $P'=0.75$, $Q'=-1.65$, obtained by van der Kraan and Buschow for binary amorphous iron alloys, we found $\delta_{IS_{\max}}=0.473$ mm/s. The large difference between $\delta_{IS_{\max}}$ and the experimental value of 0.18 ± 0.06 mm/s [reported for $x=0.001$ (Ref. 1)] could be assigned to a contribution absent in (2), the so-called R' term, which accounts for the effect of hybridization of the $3d$ electrons of Fe with the s, p electrons of Si giving rise to the formation of covalent bonds. This conclusion agrees well with the theoretical description of substitutional transition-metal impurities in Si by Hemstreet²¹ who has found that chromium and iron should form bonds with their neighboring silicon atoms. He has pointed out that the reason for this behavior could be that the atomic $3d$ and $4s$ levels are close enough in energy so that tetrahedral $s-d$ hybrids can be formed without a high expenditure of energy and that this energy can be regained by the stability obtained from the bonding configuration.

In Fig. 6 we analyze the δ_{IS} data with this model. The lower heavy line is the result of fitting expression (1) to the experimental points (up to $x=0.171$) by varying $\delta_{IS_{\max}}$. The best fit corresponded to $\delta_{IS_{\max}}=0.155$ mm/s. Though this model does not describe the experimental data as well as the logarithmic approach, it provides a clear physical meaning. It tells us that covalent effects are important and do not change much in the whole low-iron-concentration range. For this reason, bonding disruption in growing extended regions around the iron

probes does not seem to occur profusely in this range. This observation also supports that CRN-type amorphous alloys extend up to at least $x=0.17$ and suggests that iron probes occupy substitutional sites in the CRN structure. It is conceivable that formation of Fe-Fe near-neighbor pairs is not favored since it would destabilize tetrahedral bonding. The origin of the rather strong Δ_{QS} should then be looked for in the existence of trapped defects and in the long-range disorder. We have observed quite a strong contribution of the latter to the electric-field gradient in computer simulations of $A_{1-x}B_x$ cubic alloys with different degrees of chemical order.²²

The increase of the δ_{IS} in the interval $0.17 \leq x \leq 0.4$ both for implanted and coevaporated specimens indicates a continuous diminution of the R' term contribution and shows that the iron probes are located in regions of decreasing covalent character. However, as we will see below, the transformation to a metallic-type amorphous alloy does not complete up to $x=0.5$. It is interesting to note that both the δ_{IS} and Δ_{QS} measured from samples *C* and *D* ($x=0.367$ and 0.384) agree quite well with the values reported for the intermetallic compound FeSi ($\delta_{IS}=0.212$ mm/s, $\Delta_{QS}=0.499$ mm/s).²³ In fact, Fig 5 shows that the δ_{IS} and Δ_{QS} have the same correlation for implanted and evaporated samples and for this compound in this composition range. This correlation suggests that the short-range order around the iron probes in the amorphous phase becomes similar to the Fe local surroundings in the intermetallic FeSi. Actually, the number atomic density is larger in FeSi than in the diamond-like CRN structure but smaller than in the DRP one, and therefore formation of FeSi short-range order would not be inconsistent with the evolution of the system towards a denser structure.

On the other hand, this possibility is also supported by x-ray diffraction and extended x-ray-absorption fine-structure studies of silicide formation in iron- and cobalt-implanted silicon. No crystalline phases have been found in room-temperature Fe-implanted silicon at least for x up to 0.4.¹⁰ This has also been the case for implants performed at 350 °C, though cubic FeSi has been detected by x-ray diffraction for iron peak concentrations between 0.45 and 0.53.⁹ CoSi, with the same *B20* structure as FeSi, and related local structures, have been readily obtained after high dose Co implants into Si at room temperature,¹⁰ 100 °C, and 350 °C.²⁴ From these results two conclusions can be drawn: (i) These structures can develop inside or from the CRN structure, and (ii) they are stable under irradiation.

Based on the similar evolution of the δ_{IS} measured from implanted and evaporated systems in the medium composition range, we will extend our analysis to the higher x region. The upper bold curve in Fig. 6 represents the δ_{IS} values predicted by Eq. (2) using the parameters P' and Q' determined by van der Kraan and Buschow¹⁷ for amorphous iron alloys, i.e., for

$\delta_{IS_{max}}=0.473$ mm/s. This curve follows strikingly well the experimental results for $x \geq 0.5$. Since in Eq. (2) there is no term that accounts for covalency effects, these must be absent in this x range. This means that the system turns metallic, which supports its description as a DRP amorphous structure.

CONCLUSIONS

Based on the reasonable agreement between δ_{IS} data obtained from ion-implanted and from coevaporated samples, it is possible to analyze both types of systems together. It is concluded that there exist three differentiated composition ranges for $x \leq 0.17$, $0.17 < x \leq 0.5$, and $x > 0.5$.

Using the model of Miedema and van der Woude for the δ_{IS} with the parameters determined by van der Kraan and Buschow for binary iron amorphous alloys, the three x ranges can be described as follows.

(i) A silicon-rich range, where covalency effects are important and constant over the whole x interval. This situation agrees with previous descriptions of the system as a diamond-type CRN amorphous alloy. In addition, it suggests that iron occupies substitutional sites in the CRN structure. No tetrahedral bonding disruption in extended regions around the probes can be inferred from the δ_{IS} evolution.

(ii) An intermediate composition range where the degree of covalency decreases continuously until it finally vanishes. This situation may be due to the formation of Fe-Fe near-neighbor pairs driven by the increasing iron concentration. This process would reduce bonding strength and induce a transformation towards a more metallic and symmetric amorphous structure. Taking into account the values of δ_{IS} and Δ_{QS} for $x \cong 0.4$ as well as the correlation between these two quantities in this region, a short-range order alike to the local structure around the Fe sites in the cubic intermetallic FeSi is suggested.

(iii) An iron-rich region, where the results are well described using the parameters P' and Q' determined by van der Kraan and Buschow. From this observation it is concluded that the system becomes metallic, which supports the description of the short-range order as of DRP type.

ACKNOWLEDGMENTS

We would like to thank C. H. Koch and Professor H. C. Hayden for their technical assistance with the ion implanter. We are also grateful to Professor Q. Kessel for his help with the Van der Graaff accelerator. Finally, we would like to acknowledge Professor J. I. Budnick for encouraging discussions. This work was partially supported by Consejo Nacional de Investigaciones Científicas y Tecnológicas de la República Argentina.

- ¹B. D. Sawicka, J. Sawicki, and J. Stanek, *J. Phys. (Paris) Colloq.* **37**, C6-379 (1976).
- ²G. Weyer, G. Grebe, A. Kettschau, B. I. Deutch, A. Nylandsted Larsen, and O. Holk, *J. Phys. (Paris) Colloq.* **37**, C6-893 (1976).
- ³S. Damgaard, J. W. Petersen, and G. Weyer, *J. Phys. (Paris) Colloq.* **41**, C1-427 (1980).
- ⁴J. A. Sawicki, B. D. Sawicka, S. Lazarski, and E. Maydell-Ondrusz, *Phys. Status Solidi B* **57**, K143 (1973).
- ⁵J. Sawicki, B. Sawicka, J. Stanek, and J. Kowalski, *Phys. Status Solidi B* **77**, K1 (1976).
- ⁶G. Lagouche, I. Dezi, M. van Rossum, J. De Bruyn, and R. Coussement, *Phys. Status Solidi B* **89**, K17 (1978).
- ⁷B. D. Sawicka and J. A. Sawicki, *Phys. Lett.* **64A**, 311 (1977).
- ⁸Ph. Mangin, G. Marchal, B. Rudmacq, and Chr. Janot, *Philos. Mag.* **36**, 643 (1977).
- ⁹F. Namavar, F. H. Sánchez, J. I. Budnick, A. Fasihuddin, and H. C. Hayden, in *Beam-Solid Interactions and Transient Processes*, edited by M. O. Thompson, S. T. Picraux, and J. S. Williams, MRS Symposia Proceedings No. 74 (Materials Research Society, Pittsburg, 1987), p. 487.
- ¹⁰F. H. Sánchez, F. Namavar, J. I. Budnick, A. Fasihuddin, and H. C. Hayden, in *Beam-Solid Interactions and Phase Transformations*, edited by H. Kurz, G. L. Olson, and J. M. Poate, MRS Symposia Proceedings No. 51 (Materials Research Society, Pittsburg, 1986), p. 439.
- ¹¹A. R. Miedema and F. van der Woude, *Physica* **100B**, 145 (1980).
- ¹²G. Marchal, Ph. Mangin, M. Piecuch, and Chr. Janot, *J. Phys. (Paris) Colloq.* **37**, C6-763 (1976).
- ¹³K. Yamakawa and F. E. Fujita, *J. Phys. (Paris) Colloq.* **40**, C2-101 (1979).
- ¹⁴M. B. Stearns, *Phys. Rev.* **147**, 439 (1966).
- ¹⁵W. E. Sauer and B. J. Reaynik, *J. Appl. Phys.* **42**, 1604 (1971).
- ¹⁶J. Vincze and J. A. Campbell, *J. Phys. F* **3**, 647 (1973).
- ¹⁷A. M. van der Kraan and K. H. J. Buschow, *Phys. Rev. B* **27**, 2693 (1983).
- ¹⁸R. Ingalls, F. van der Woude, and G. A. Sawatzky, in *Mossbauer Isomer Shifts*, edited by G. K. Shenoy and F. W. Wagner (North-Holland, Amsterdam, 1978), p. 415.
- ¹⁹B. D. Sawicka, J. A. Sawicki, J. Stanek, T. Tyliczszak, and J. Kowalski, *Phys. Status Solidi A* **56**, 451 (1979).
- ²⁰A. R. Miedema, P. F. de Châtel, and F. R. de Boer, *Physica* **100B**, 1 (1980).
- ²¹L. A. Hemstreet, *Phys. Rev. B* **15**, 834 (1977).
- ²²F. H. Sánchez and M. B. Fernández van Raap (unpublished).
- ²³K. Vojtyzechovsky and T. Zemcik, *Czech. J. Phys. B* **24**, 171 (1974).
- ²⁴Heng-Quan Tan, J. I. Budnick, F. H. Sánchez, G. Tourillon, F. Namavar, and H. C. Hayden, *Phys. Rev. B* **40**, 6368 (1989).